



IX

**INTERNATIONAL WORKSHOP
ON**

MICROWAVE DISCHARGES: Fundamentals and Applications

September 7-11, 2015
Cordoba (Spain)

Edited by
Antonio Gamero
Antonio Sola



PROCEEDINGS

Microwave Discharges: Fundamentals and Applications. – Córdoba : UCOPress. Cordoba University Press, 2015

Co-Editors: Antonio Gamero & Antonio Sola

Edita: UCOPress. Editorial Universidad de Córdoba
Campus Universitario de Rabanales
Ctra. Nacional IV, km. 396
14071 – Córdoba, Spain

<http://www.uco.es/ucopress>
ucopress@uco.es

Imprime: Gráficas Minerva de Córdoba, S.L.
Tel. 957 32 22 22

ISBN: 978-84-9927-187-3

DL: CO 2010-2015

© UCOPress

© Authors

100% Ecologic paper

All rights reserved. No part of this book may be reproduced, translated, stored in any retrieval system, nor transmitted in any form without written permission from the Publisher

Printed in Spain

COMPUTER MODELING OF A MICROWAVE DISCHARGE USED FOR CO₂ SPLITTING

A. Bogaerts, A. Berthelot, S. Heijkers and T. Kozak¹

Research Group PLASMANT, University of Antwerp, Department of Chemistry, Universiteitsplein 1, B-2610 Antwerp, Belgium

¹Department of Physics and NTIS, European Centre of Excellence, University of West Bohemia, Univerzitní 8, 30614 Plzeň, Czech Republic

Abstract. In this paper, we present a number of models which we developed with the aim to describe CO₂ splitting in a microwave plasma. A detailed zero-dimensional chemical kinetics model describes the underlying plasma chemistry of CO₂ splitting, with special emphasis on the behavior of the CO₂ vibrational levels, as they play a very important role in the splitting process in a microwave plasma. Besides a pure CO₂ plasma, the influence of N₂ on the CO₂ splitting is also investigated, showing that the N₂ vibrational levels contribute to a large extent to the CO₂ splitting. Furthermore, a two-dimensional model for a microwave plasma is developed, but due to the large number of reactions playing a role in a CO₂ plasma, and thus the significant computation time, this model is in first instance developed for argon. Some typical results are illustrated, such as the electron density and temperature, the gas temperature and electric field distribution.

1. INTRODUCTION

Recently, plasma technology is gaining increased interest for the conversion of CO₂ into value-added chemicals or fuels [1,2]. Microwave (MW) discharges are particularly interesting in this respect, because of their high energy efficiency. Indeed, already in 1983, a very high energy efficiency (i.e., the highest up to now) of 90% was reported [3]. This was, however, at very specific conditions, i.e., supersonic gas flow and reduced pressure (~100-200 Torr), and a pressure rise to atmospheric pressure, which is desirable for industry, yields a drop in energy efficiency to 40% [1]. More recently, again high energy efficiencies are being reported, i.e., up to 55% [4], again for reduced pressure and supersonic flow. Latest results, however, indicate that with a special (reverse) vortex flow, energy efficiencies up to 50% are feasible even at atmospheric pressure [5].

The reason for the high energy efficiency for CO₂ splitting in MW discharges is that CO₂ is very efficiently excited to the vibrational levels in a MW plasma, and these vibrational levels provide a very efficient dissociation pathway [1]. We have developed a detailed vibrational kinetics model for CO₂, to better understand the underlying processes [6,7]. This model will be briefly explained here, and some typical results will be presented. Furthermore, we have extended this model to a CO₂/N₂ mixture [8], as real industrial exhaust gases are typically not pure CO₂, but contain a significant fraction of N₂. This model allows to elucidate the role of N₂ in the CO₂ splitting process, as will be illustrated below. The aim is now to include the CO₂ vibrational kinetics model in a 2D model for a MW plasma. However, introducing the entire model would yield a too long calculation time. Therefore, the detailed CO₂ model first needs to be reduced, to keep only the most important species and chemical reactions. This process is currently under development. Before developing this model in CO₂, we already set up a 2D model for a MW plasma in argon, and some characteristic results will also be presented here.

2. EXPLANATION OF THE MODELS

2.1. Vibrational kinetics model for pure CO₂

We developed a zero-dimensional (0D) chemical reaction kinetics model, which is the most appropriate model for describing a detailed plasma chemistry. This model consists of solving balance equations for the species densities, based on production and loss rates, as determined by the chemical reactions:

$$\frac{dn_i}{dt} = \sum_j \left\{ \left(a_{ij}^{(2)} - a_{ij}^{(1)} \right) k_j \prod_l n_l^{a_{lj}^{(1)}} \right\} \quad (1)$$

In this equation, $a_{ij}^{(1)}$ and $a_{ij}^{(2)}$ are the stoichiometric coefficients of species i , at the left and right hand side of a reaction j , respectively, n_l is the species density at the left-hand side of the reaction, and k_j is the rate coefficient of reaction j (see below).

Such a balance equation needs to be solved for each species included in the model, i.e., different types of molecules, radicals, ions, excited species, as well as the electrons. The different species taken into account in our CO₂ vibrational kinetics model, are listed in Table 1.

Table 1. Overview of the species included in the CO₂ model.

Molecules	Charged species	Radicals	Excited species
CO ₂ , CO	CO ₂ ⁺ , CO ₄ ⁺ , CO ⁺ , C ₂ O ₂ ⁺ , C ₂ O ₃ ⁺ , C ₂ O ₄ ⁺ , C ₂ ⁺ , C ⁺ , CO ₃ ⁻ , CO ₄ ⁻	C ₂ O, C, C ₂	CO ₂ (Va, Vb, Vc, Vd), CO ₂ (V1-V21), CO ₂ (E1, E2), CO(V1-V10), CO(E1-E4)
O ₂ , O ₃ ,	O ⁺ , O ₂ ⁺ , O ₄ ⁺ , O ⁻ , O ₂ ⁻ , O ₃ ⁻ , O ₄ ⁻	O	O ₂ (V1-V4), O ₂ (E1-E2)
	electrons		

The symbols ‘‘V’’ and ‘‘E’’ between brackets for CO₂, CO and O₂ represent the vibrationally and electronically excited levels of these species, respectively. Details about these notations can be found in [6,7]. We will only briefly elaborate on the CO₂ vibrational levels, as they are the most important. The CO₂ molecule exhibits three vibration modes, i.e., symmetric stretching, asymmetric stretching and bending. The bending mode is doubly degenerate as a result of the linear symmetry of the molecule. It is generally accepted [1] that the asymmetric stretch mode provides the most important channel for dissociation, because of the following reasons: (i) the typical electron temperatures of 1-3 eV mainly yield excitation of this mode, (ii) the relaxation rate constants of the asymmetric mode are lower than those of the symmetric stretching and bending modes, and (iii) vibrational energy exchange among the asymmetric mode levels (VV relaxation) is very fast, yielding population of the highly excited states of this mode. Therefore, the highly excited asymmetric mode levels are considered very important for dissociation of CO₂ through step-by-step vibrational excitation. Taking this into account, our model includes all the asymmetric mode levels up to the dissociation energy of 5.5 eV (i.e., 21 levels, denoted by numbers (V1-V21) in Table 1 above). On the other hand, only 4 effective low-lying symmetric stretching and bending mode levels are included (denoted by Latin letters (Va-Vd) in Table 1). The energy diagram of the CO₂ levels included in the model can be found in [6,7].

All the species will chemically react with each other. Hence, a large number of chemical reactions is incorporated in this model, including electron impact reactions, electron-ion recombinations, ion-ion, ion-neutral and neutral-neutral reactions. Of special interest are the state-specific vibration-translation (VT) and vibration-vibration (VV) relaxation reactions, as well as the effect of vibrational excitation on other chemical reactions. All details about these chemical reactions, as well as the corresponding rate coefficients and the theories behind it in order to estimate these values, can be found in [6].

The above balance equations yield the time-evolution of the species densities, averaged over the plasma reactor volume. Indeed, this 0D model only accounts for time-variations, while spatial variations, due to transport in the plasma, are not considered. However, based on the gas flow rate,

we can translate the time-variation into a spatial variation, i.e., as a function of distance travelled through the plasma reactor. In this way, we can even account for spatial variations of input power or gas temperature inside the plasma reactor. Indeed, the power deposition in a MW plasma is highest at the position of the waveguide, and as a result of this, the gas temperature will increase as a function of position. This can be accounted for in this 0D model.

Besides the species densities, also the average electron energy is calculated in this model, based on an energy balance equation, again with energy source and loss terms as defined by the chemical reactions. The average electron energy is used to calculate the energy-dependent rate coefficients of the electron-induced processes, such as ionization, excitation and dissociation. The rate coefficients of the other chemical reactions, i.e., between the neutral species or ions, depend on the gas temperature and are calculated from Arrhenius equations, using data adopted from literature.

2.2. Vibrational kinetics model for a CO₂-N₂ mixture

Real industrial gas flows are typically not pure CO₂, but mixed with other gases and impurities. In most cases, N₂ is the most important component. Therefore, it is also crucial to investigate how the CO₂ conversion and energy efficiency are affected by the presence of N₂, and moreover, which products (e.g., useful or harmful NO_x compounds) would be formed in this gas mixture. We have thus extended the above model to a CO₂/N₂ mixture, by incorporating also the N₂ vibrational levels, which turn out to be important for populating the CO₂ vibrational levels in a MW plasma [8]. We took into account 14 N₂ vibrational levels (V1-14), as well as a number of electronically excited levels of these species, for which the detailed notations are given in Table 2. Details about this model and the chemical reactions can all be found in [8].

Table 2. Overview of the extra species added to the pure CO₂ model (see Table 1), in order to describe the CO₂/N₂ mixture.

Molecules	Charged species	Radicals	Excited species
N ₂	N ⁺ , N ₂ ⁺ , N ₃ ⁺ , N ₄ ⁺	N	N ₂ (V1-V14), N ₂ (C ³ Π _u), N ₂ (A ³ Σ _u ⁺), N ₂ (a ¹ Σ _u ⁻), N ₂ (B ³ Π _g), N(2D), N(2P)
NO, N ₂ O, NO ₂ , NO ₃ , N ₂ O ₅	NO ⁺ , N ₂ O ⁺ , NO ₂ ⁺ , NO ⁻ , N ₂ O ⁻ , NO ₂ ⁻ , NO ₃ ⁻ , N ₂ O ₂ ⁺	CN, NCO, ONCN, C ₂ N ₂ , NCN	

2.3. 2D model for a MW plasma

We developed a 2D model for a MW plasma, implemented in the commercial software COMSOL Multiphysics ®. It consists of solving conservation equations for the densities of the various plasma species and for the average electron energy. The conservation equations for the species densities are again based on source and loss terms, defined by the chemical reactions. The source of the electron energy is due to heating by the electric field, and the energy loss is dictated by collisions. In addition, transport is now also included in the conservation equations. It is defined by diffusion, migration in the electric field (for the charged species) and convection due to the gas velocity (see below).

The electromagnetic (EM) field distribution is obtained from the Maxwell equations. Furthermore, the gas temperature and the gas flow behavior are calculated with a heat transfer equation and the Navier-Stokes equations. The fluid (plasma) model and the models for gas flow and gas heating are combined into a multiphysics model: the calculated gas velocity is inserted in the transport equations of the plasma species, while the gas temperature defines the gas density profile, and both the gas temperature and density determine the chemical reaction rates.

As mentioned in the Introduction, we first developed this model for an argon plasma, to limit the calculation time. In the next step, this model will be extended to CO₂. The argon model considers the following species: Ar atoms, Ar⁺ and Ar₂⁺ ions, Ar(4s), which is a lumped excitation level comprising

the 4 individual 4s levels, a lumped $Ar(4p)$ level, and Ar_2^* , which includes $Ar_2(^1\Sigma_u^+)$ and $Ar_2(^3\Sigma_u^+)$ excited molecules. The reactions between the different species, as well as the transport parameters are the same as in [9]. The electron energy distribution function is pre-calculated using Bolsig+ [10] and is used to calculate the rate coefficients of electron impact collisions for different pressure regimes.

A schematic diagram of the 2D-axisymmetric computational domain is shown in Figure 1. It is based on the setup used in [11,12].

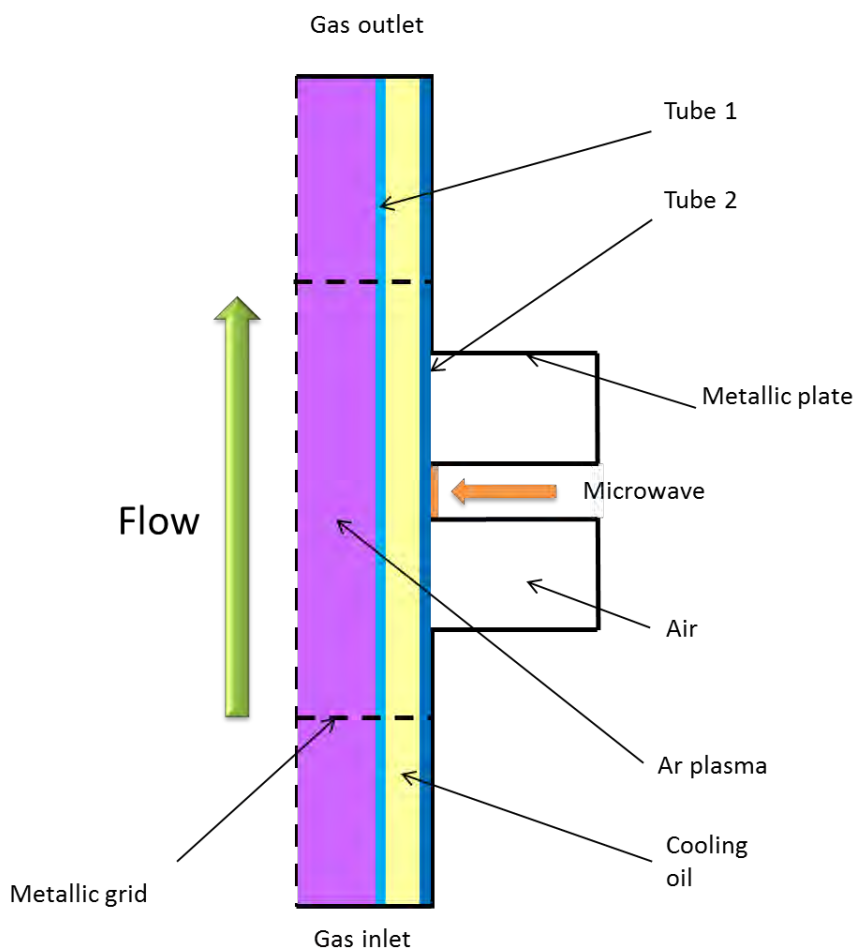


Figure 1. Schematic diagram of the MW plasma, assumed in the model.

By comparing the calculated EM field distribution in a 3D geometry and in a 2D-axisymmetric geometry, we have made sure that a 2D-axisymmetric model could accurately reproduce the EM field created in this configuration.

3. RESULTS

3.1. Vibrational kinetics model for pure CO_2

The 0D model allows to calculate the densities of all species as a function of time, which can be translated to a variation as a function of distance travelled through the reactor, by means of the gas flow rate, as mentioned above. By comparing the CO_2 density at the inlet and outlet of the MW plasma (or in other words: at the beginning and the end of the calculations), we can obtain the CO_2 conversion. The latter, in combination with the specific energy input (SEI), as obtained from the gas flow rate and applied power, yields the energy efficiency of CO_2 conversion. Both the CO_2 conversion and energy efficiency are plotted as a function of SEI in Figure 2, for a reduced pressure of 2660 Pa, as used in the experiments

of [11,12], and a gas temperature, self-consistently calculated in the model as a function of time (or distance in the reactor), yielding values up to 1000 K [7].

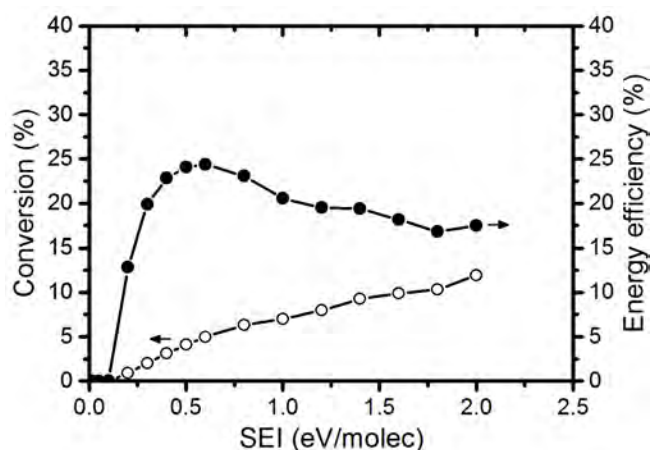


Figure 2. Calculated CO₂ conversion (open symbols, left axis) and energy efficiency (solid symbols, right axis), as a function of SEI, at a pressure of 2660 Pa and a self-consistently calculated gas temperature, reaching values up to 1000 K.

The conversion rises as a function of SEI, which is logical, because more energy goes into the system, which can be used for the CO₂ splitting. At an SEI of 2 eV/molec, the CO₂ conversion reaches about 12%. The energy efficiency reaches its maximum (around 25%) at an SEI around 0.6 eV/molec, which is in good agreement with the theoretical and experimental results presented in [1], although in that case, energy efficiencies up to 80-90% were reported. Below, we will discuss the major effects that limit the maximum energy efficiency in our case.

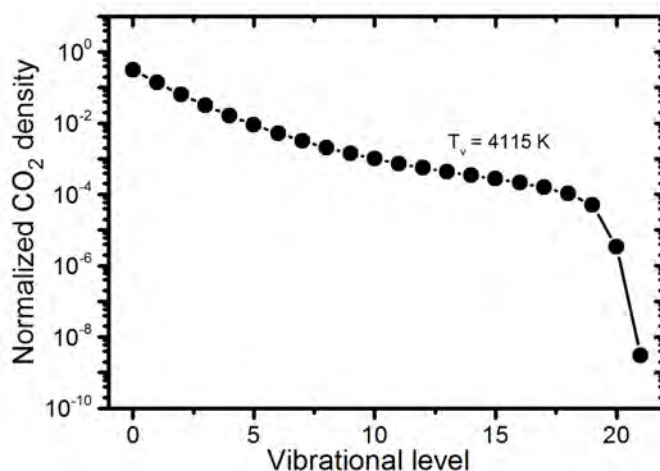


Figure 3. Normalized vibrational distribution function of the asymmetric mode levels of CO₂, at an SEI of 0.6 eV/molec, taken at the time of maximum vibrational temperature.

Figure 3 illustrates the vibrational distribution function of the CO₂ asymmetric mode levels (i.e., the mode which is most important for CO₂ splitting; cf. above), for an SEI of 0.6 eV/molec. It is clear that the vibrational distribution drops quite smoothly, yielding a vibrational temperature of 4115 K. Although the population of the highest vibrational levels is much lower than the ground state density, they still play an important role in the CO₂ splitting process, which explains why the CO₂ conversion and energy efficiency in a MW plasma are much higher than in a dielectric barrier discharge (DBD) plasma [6]. Indeed, while in a DBD reactor, electron impact excitation from the CO₂ ground state, followed by dissociation, is mainly responsible for CO₂ splitting [1,13], in the MW plasma, the CO₂ splitting predominantly proceeds by electron impact vibrational excitation of the lowest vibrational levels, followed by vibrational-vibrational (VV) collisions, gradually populating the higher vibrational levels, which then lead to dissociation of the CO₂ molecule, and the latter is a more energy-efficient process.

Our model also allows to identify the discharge conditions that favour the highest energy efficiency for CO₂ conversion. The highest value reached in our calculations was around 32%, and was obtained at an SEI in the range of 0.4-1.0 eV/molec and a reduced electric field in the range of 50-100 Td [7]. Moreover, our calculations predict that a shorter residence time favours a higher energy efficiency, because in that case the time for vibration-translation (VT) relaxation, which depopulates the vibrational levels, is longer than the residence time of the gas within the plasma. This is in agreement with the fact that the highest energy efficiencies were reported at supersonic flow conditions [3,4].

The best energy efficiencies obtained experimentally in a MW plasma at moderate pressure were 80% in subsonic flow, and up to 90% in supersonic flow conditions [1,3]. These results were obtained in 1983, and since then, such high values have not been obtained anymore. However, recently, energy efficiencies as high as 55% were obtained with a MW plasma, again at moderate pressure and supersonic flow conditions [4], which is still higher than the values obtained by our model. Thus, to better understand the limitations in the energy efficiency, we have analysed how the vibrational energy of CO₂ is consumed by individual reactions. Our model predicts that up to 60% of the energy available in the CO₂ vibrational levels can be used for CO₂ dissociation, at least at high enough electron density (order of 10²⁰ m⁻³ at a pressure of 100 Torr) [7]. The remaining fraction of the energy is largely lost by VT relaxation, which gives rise to the gas heating. Vice versa, because a higher gas temperature gives rise to higher VT relaxation rates, it is desirable to keep the gas temperature as low as possible, to minimize VT relaxation losses in the vibrational population. This is also one of the reasons why the energy efficiency drops upon increasing gas pressure, because of the increasing V-T relaxation processes. One way to reduce this effect is by using a fast gas flow, as mentioned above.

We have also looked at the underlying plasma chemistry of CO₂ splitting in a MW plasma, to elucidate how the CO₂ conversion efficiency can be further enhanced. Our calculations predict that the energy efficiency is strongly affected by the reaction chemistry of the O atoms formed by CO₂ splitting. When these O atoms would be entirely used for further dissociation of CO₂ (i.e., CO₂ + O → CO + O₂) instead of recombining with other O atoms into O₂, the highest energy efficiency can be obtained. The above dissociation reaction indeed seems to limit the attainable energy efficiency, as it is characterized by a quite high activation energy (1.43 eV). When artificially lowering this activation energy to the theoretical minimum of 0.35 eV (dictated by the reaction enthalpy), the rate of this reaction increases by 6 orders of magnitude, and the calculated energy efficiency of CO₂ splitting would rise from 30% to 52%, which is close to the highest values reported by Goede et al. [4]. Hence, this indicates the limiting factor of this further dissociation reaction in determining the overall energy efficiency, and therefore, we should look for conditions that can enhance this reaction, at the expense of the recombination of two O atoms into O₂.

3.2. Vibrational kinetics model for a CO₂-N₂ mixture

Figure 4 illustrates the absolute and effective CO₂ conversions and energy efficiency for CO₂ conversion, as a function of N₂ content in the gas mixture, for three different values of power density investigated, i.e., 30, 50 and 80 W/cm³. Besides the calculated values, also experimental data are presented, which were obtained from Silva and colleagues, in a surfaguide-type microwave discharge, at a frequency of 915 MHz in a double-walled quartz tube with 14 mm inner diameter and about 20 cm length [8]. The whole system was surrounded by a grounded aluminum grid to prevent any leak of microwave radiation into outer space.

The absolute conversion (Figure 4(a)) generally increases with N₂ fraction, both in the model and the experiments, except for a slight drop between 0 and 10% N₂ in the model results. This indicates that N₂ has a beneficial effect on the conversion (see below). The effective CO₂ conversion (Figure 4(b)), however, drops upon increasing N₂ fraction, because there is less CO₂ initially present in the gas mixture. The CO₂ conversion is quite high (i.e., 10-80% absolute conversion and 5-53% effective conversion, depending on power and N₂ fraction) and it clearly increases with rising power density, as expected.

The energy efficiency for CO₂ conversion (Figure 4(c)) more or less follows the trend of the effective CO₂ conversion, from which it is calculated. It is in the order of 8-15%, slightly dropping upon higher N₂ fraction, except at the highest N₂ contents, where it drops more significantly to 3%. Furthermore, the calculated values drop from 0 to 10% N₂ fraction. This trend was not observed in the experiments, but the latter might be attributed to a rather high measurement error in this case [8]. The maximum obtained calculated energy efficiency (i.e., 21% at 80 W/cm³) is obtained for the pure CO₂ case (cf. also the values reported in section 3.1 above).

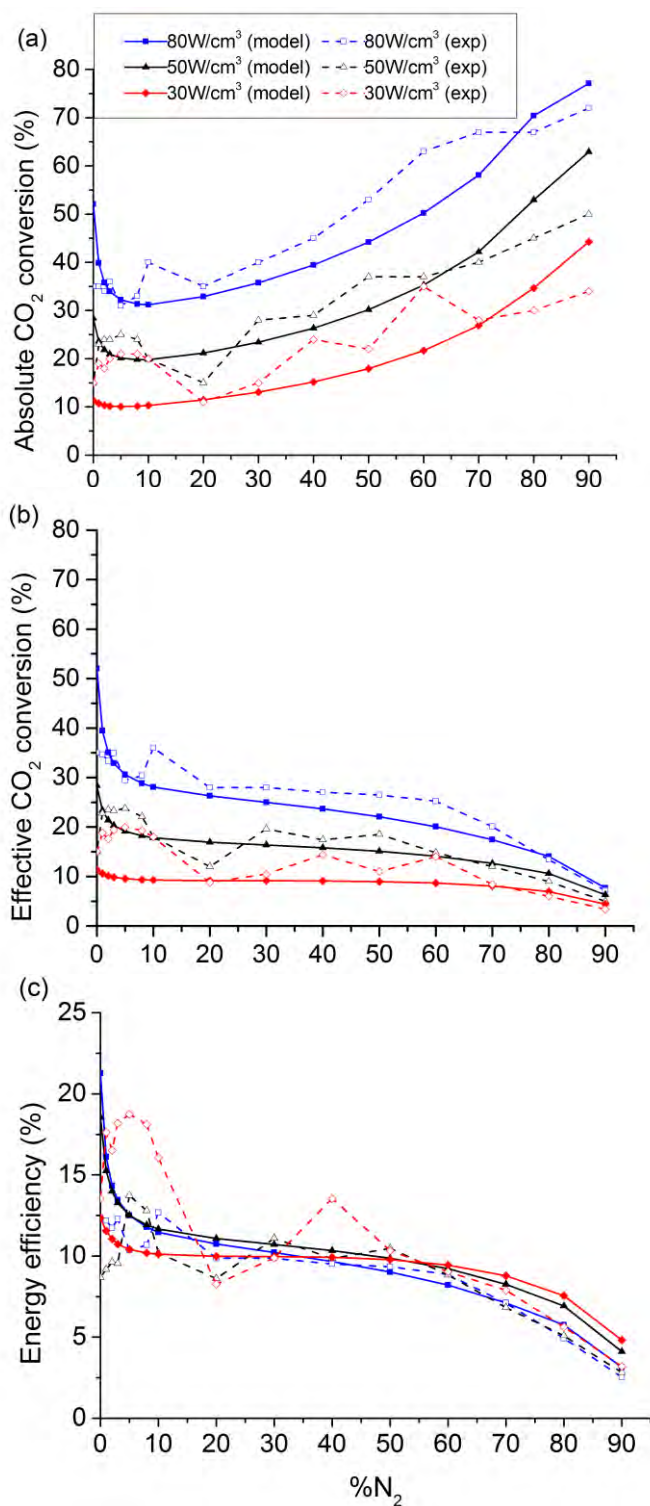


Figure 4. Calculated (solid lines) and measured (dashed lines) absolute (a) and effective (b) CO₂ conversion, and energy efficiency (c), as a function of N₂ fraction in the gas mixture, for three different power densities, a pressure of 2660 Pa, and a residence time of 9.13 ms.

In general, reasonable agreement (~30%) is obtained between the calculations and experiments. This indicates that the plasma chemistry and vibrational kinetics occurring in the microwave plasma are quite realistically described in our model. Thus, the model can be used to explain the observed trends. For this purpose, we have analyzed the destruction and formation processes of both CO₂ and N₂, as well as their vibrational distribution functions (VDFs). The major destruction process for CO₂ is dissociation of vibrationally excited CO₂ upon collision with any molecule or atom in the plasma, especially at the higher power densities. At the lowest power density investigated and low N₂ fractions, electron impact dissociation from CO₂, both in the ground state and vibrationally excited levels, are more important. Because dissociation from the ground state requires a significant amount of energy, this explains the somewhat lower energy efficiency obtained at the lowest power density and low N₂ fractions.

We have also calculated the VDFs of CO₂ and N₂ (see [8] for more details). The vibrational levels of CO₂ are important at all power densities investigated, especially at high N₂ fractions. Our calculations reveal that the lower CO₂ vibrational levels are mainly populated by electron impact vibrational excitation at low N₂ fractions, while at high N₂ fractions, VV relaxation with N₂ becomes increasingly important. Subsequently, VV relaxation with CO and CO₂ will (partially) convert these lower levels into the higher vibrational levels, which are essential for energy efficient CO₂ splitting. This illustrates the important role of N₂ in populating the CO₂ vibrational levels, and explains the higher CO₂ conversion upon addition of N₂. In general, we can conclude that both the CO₂ and N₂ vibrational levels play a very important role in the (energy-efficient) CO₂ conversion.

Finally, our calculations predict that several NO_x compounds are produced in the CO₂/N₂ plasma, especially NO, NO₂ and N₂O. Although their concentrations remain in the ppm range, this is still significant, since they give rise to several environmental problems. N₂O is also a greenhouse gas, with a global warming potential 300 times higher than for CO₂, while NO and NO₂ are responsible for acid rain and the formation of ozone and a wide variety of toxic products. These results indicate that it might be important to separate the CO₂ gas from N₂ impurities (or gas fractions) before plasma treatment, to avoid the formation of NO_x compounds. On the other hand, if the NO_x concentrations would be sufficiently high, we could even make profit of them, in terms of nitrogen-fixation into the formation of value-added compounds.

3.3. 2D model for a MW plasma

The 2D model yields the densities of all plasma species, the average electron energy and the gas temperature, all as a function of position in the plasma, as well as the electric field distribution and the gas flow pattern in the MW reactor. Figure 5 illustrates the calculated electron density (a), electron temperature (b), gas temperature (c) and MW electric field (d) distributions, for a pressure of 1000 Pa, a gas flow rate of 500 sccm, a frequency of 2.45 GHz and a power of 100 W.

The electron density reaches a maximum value of $9 \times 10^{19} \text{ m}^{-3}$ in front of the waveguide, and decreases more or less linearly from the center to the end of the plasma, while at the same time, it exhibits a wave-like pattern, as a result of resonance due to the metallic grids. The electron density is fairly constant in the entire plasma volume, at least within the region confined by the metallic grids (which are located at $z = 15$ and 45 cm), and exhibits a typical value of 1.2 eV. The gas temperature shows a maximum of 1400 K, located at the position of the waveguide, which is the position of maximum power deposition, and it drops to about 400 K in the flowing afterglow. The effect of the gas flow is clearly visible in figure 5(c). Indeed, the gas is flowing from the bottom to the top, and the gas temperature in the region $z = 50\text{-}60$ cm (i.e., the flowing afterglow) is somewhat higher than in the region $z = 0\text{-}10$ cm. Finally, the electric field due to the MW power is characterized by a pronounced maximum near the walls, indicating the skin effect, and low values in the center of the plasma. Moreover, the metallic grids clearly prevent any leakage of the electric field outside of the cavity. All these results are in reasonable agreement with data from literature, for a similar setup and a similar pressure [14].

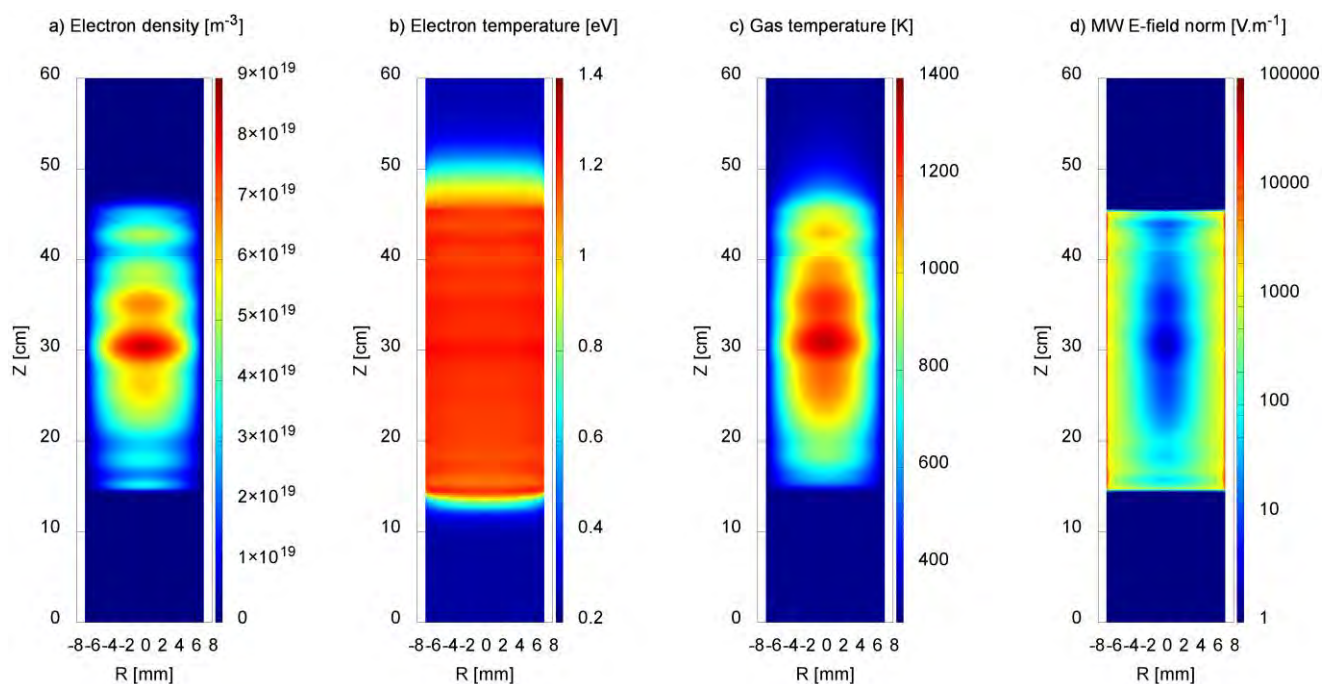


Figure 5. Calculated profiles of electron density in m^{-3} (a), electron temperature in eV (b), gas temperature in K (c) and MW electric field in V/m (d), at 1000 Pa, a gas flow rate of 500 sccm, a frequency of 2.45 GHz and a power of 100 W.

As mentioned, in the near future, this model will be extended to a CO_2 plasma, so that, besides the above quantities, also information can be obtained about the reactive species densities (including the vibrational levels), the CO_2 conversion and energy efficiency.

4. CONCLUSION

We presented some modeling results for a MW plasma, for the application of CO_2 splitting. A 0D chemical kinetics model is developed to describe the behavior of the vibrational levels and their role in energy-efficient CO_2 conversion. The calculated CO_2 conversion is found to rise upon increasing SEI, while the energy efficiency reaches a maximum at an SEI around 0.6 eV/molec. The model predicts that VT relaxation is the limiting process for energy-efficient CO_2 splitting, and this limiting factor can be reduced by working with higher gas flow rates (so that the time for VT relaxation is longer than the gas residence time) and reduced temperature (limiting the rates of VT relaxation). Also, the reaction chemistry of the O atoms formed by CO_2 splitting is limiting the energy efficiency. When these O atoms could be entirely used for further dissociation of CO_2 (i.e., $\text{CO}_2 + \text{O} \rightarrow \text{CO} + \text{O}_2$) instead of recombining with other O atoms into O_2 , the highest energy efficiency would be obtained.

We have also extended this CO_2 vibrational model to a CO_2/N_2 mixture, including also the N_2 vibrational levels, and the calculated CO_2 conversion and energy efficiency are compared with experiments, performed at the University of Mons, for different values of power density and a wide range of CO_2/N_2 gas mixing ratios, and reasonable agreement is obtained. The model explains how N_2 populates the CO_2 vibrational levels, and thus contributes to a higher CO_2 conversion.

Finally, we presented a self-consistent 2D fluid plasma model of a surfaguide discharge. This model is in first instance developed for argon, but will be extended to CO_2 . Typical results of this model include the electron density and temperature profiles, the electric field distribution and the gas temperature profile. These results are in reasonable agreement with literature data.

5. ACKNOWLEDGMENTS

We would like to thank T. Silva, N. Britoun, Th. Godfroid and R. Snyders (Université de Mons and Materia Nova Research Center) for providing the experimental data for the CO_2/N_2 mixture.

Furthermore, we acknowledge financial support from the IAP/7 (Inter-university Attraction Pole) program ‘PSI-Physical Chemistry of Plasma-Surface Interactions’ by the Belgian Federal Office for Science Policy (BELSPO), the Francqui Research Foundation and the EU-FP7-ITN network “RAPID”.

REFERENCES

1. Fridman A. Plasma Chemistry, Cambridge University Press, Cambridge, 2008.
2. Aerts R., Somers W. and Bogaerts A. ChemSusChem., 2015, 8, 702.
3. Asisov R. I., Givotov V. K., Krashennnikov E. G., Potapkin B. V., Rusanov V. D. and Fridman A. Sov. Phys., Doklady, 1983, 271, 94.
4. Goede, A. P. H., Bongers W. A., Graswinckel M. F., van de Sanden M. C. M., Leins M, Kopecki J., Schulz A. and Walker M. EPJ Web of Conferences, 3rd Eur. Energy Conference, 2013.
5. Bongers W., Proc. of the International Symposium on Plasma Chemistry, Antwerp, 2015.
6. Kozák T. and Bogaerts A. Plasma Sources Sci. Technol., 2014, 23, 045004.
7. Kozák T. and Bogaerts A. Plasma Sources Sci. Technol., 2015, 24, 015024.
8. Heijkers S., Snoeckx R., Kozák T., Silva T., Godfroid T., Britun N., Snyders R. and Bogaerts A. J. Phys. Chem. C, 2015, 119, 12815.
9. Kolev St. and Bogaerts A. Plasma Sources Sci. Technol., 2015, 24, 1.
10. Hagelaar G. J. M. and Pitchford L. C. Plasma Sources Sci. Technol., 2005, 14, 4.
11. Britun N., Godfroid T. and Snyders R. Plasma Sources Sci. Technol., 2012, 21, 035007.
12. Silva T., Britun N., Godfroid T. and Snyders R. Plasma Sources Sci. Technol., 2014, 23, 2.
13. Aerts R., Martens T. and Bogaerts A. J. Phys. Chem. C 2012, 116, 23257.
14. Boisse-Laporte C., Granier A., Dervisevic E., Leprince P. and Marec J. J. Phys. D: Appl. Phys. 1987, 20, 197.